

Effects of relativity and configuration interaction on dielectronic recombination of hydrogenlike ions

Mau Hsiung Chen

*High Temperature Physics Division, University of California, Lawrence Livermore National Laboratory,
Livermore, California 94550*

(Received 30 March 1988)

Effects of configuration interaction and relativity on the dielectronic satellite spectra and total dielectronic rate coefficients for the hydrogenlike ions were investigated. The calculations were carried out for the intermediate autoionizing states of the $2l2l'$ and $2l3l'$ configurations by using relativistic and nonrelativistic Hartree-Fock models. The effect of relativity has been found to change the Auger rates by as much as a factor of 18 at $Z=54$. The inclusion of the Breit interaction in calculations of the Auger matrix elements could change the Auger rates by as much as a factor of 4 for the Xe^{52+} ion. The effect of configuration interaction has been found to alter some of the transition rates by a factor of 2. The dielectronic satellite spectra become much more complex due to the inclusion of configuration interaction and intermediate coupling. The effects of relativity and configuration interaction, however, have been found to change the total dielectronic recombination coefficients by amounts less than 20% and a few percent, respectively, for the Cr^{23+} and Xe^{53+} ions.

I. INTRODUCTION

Dielectronic recombination (DR) is an important recombination process for high-temperature plasmas in connection with x-ray laser experiments, fusion research, and astrophysics. Knowledge of DR coefficients is essential in the determination of the ionization balance and the plasma kinetics.^{1,2} Dielectronic satellite lines observed in the emission spectra can be used in the plasma diagnostics.

There have been many calculations for DR satellite lines and rate coefficients for hydrogenlike ions.³⁻⁶ However, the effects of relativity and configuration interaction on the DR satellite spectra and total DR coefficients for the hydrogenlike ions have not been explicitly studied. Especially, the role played by the Breit interaction in the calculations of dielectronic capture has not been fully investigated.

In this paper, we report on the studies of the effects of relativity and configuration interaction on the DR satellite spectra and rate coefficients by comparing the theoretical results from nonrelativistic and relativistic single-configuration and multiconfiguration Hartree-Fock calculations with and without Breit interaction. Explicit calculations were carried out for the hydrogenlike ^{10}Ne , ^{24}Cr , ^{42}Mo , and ^{54}Xe .

II. THEORETICAL METHODS

The intensity of dielectronic satellite line for low-density plasmas, in the isolated resonance approximation, can be written as⁷

$$I_i(d-f) = n_e n_i \alpha_{\text{DR}}(i, d-f), \quad (1)$$

where

$$\alpha_{\text{DR}}(i, d-f) = \frac{1}{2} \left[\frac{4\pi R}{kT} \right]^{3/2} a_0^3 F_2(d-f) \exp(-e_2/kT) \quad (2)$$

and

$$F_2(d-f) = \frac{g_d/g_i A_a(d-i) A_r(d-f)}{\Gamma_r(d) + \Gamma_a(d)}. \quad (3)$$

Here n_e and n_i represent the electron density and density of the recombining ion, respectively; g_d and g_i are, respectively, the statistical weight factors for the ionic states d and i ; R is the Rydberg energy and a_0 is the Bohr radius; $A_a(d-i)$ is the Auger rate from intermediate state d to initial state i of the recombining ion with Auger energy e_2 ; $A_r(d-f)$ is the radiative rate from state d to f ; Γ_r and Γ_a are the total radiative and Auger rates for the autoionizing state d , respectively. The velocity of the plasma electron is assumed to have a Maxwellian distribution.

The total dielectronic recombination rate coefficient can be obtained from Eqs. (2) and (3) by summing over the possible intermediate state d and the stabilized final stage f .

In the present work, the Auger and radiative rates and transition energies required in the evaluation of Eqs. (2) and (3) were calculated for each autoionizing state. The Auger transition probably is calculated from perturbation theory.^{8,9} The transition rate in a frozen-orbital approximation is given by

$$A_a = \frac{2\pi}{\hbar} \left| \left\langle \psi_f \left| \sum_{\substack{\alpha, \beta \\ (\alpha < \beta)}} V_{\alpha\beta} \right| \psi_i \right\rangle \right|^2 \rho(\epsilon). \quad (4)$$

Here $\rho(\epsilon)$ is the density of final states and $V_{\alpha\beta}$ is the

two-electron interaction operator. In the present work, $V_{\alpha\beta}$ is taken to be the Coulomb-Breit operator which, in atomic units, is given by¹⁰

$$V_{12} = \frac{1}{r_{12}} - \alpha_1 \cdot \alpha_2 \frac{\cos(\omega r_{12})}{r_{12}} + (\alpha_1 \cdot \nabla_1)(\alpha_2 \cdot \nabla_2) \frac{\cos(\omega r_{12}) - 1}{\omega^2 r_{12}}. \quad (5)$$

For purpose of comparison, we also calculate the Auger rates using the Coulomb operator, alone.

The spontaneous electric dipole ($E1$) transition probability for discrete transition $i \rightarrow f$ is given in perturbation theory by¹¹

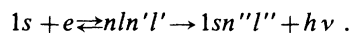
$$A_r(i-f) = \frac{2\pi}{3(2J_i + 1)} |\langle f || T_1 || i \rangle|^2. \quad (6)$$

Here, $\langle f || T_1 || i \rangle$ is the electric dipole reduced matrix element.

In the present work, the transition matrix elements in Eqs. (4) and (6) were evaluated in the framework of the multiconfiguration Dirac-Fock (MCDF) model. For detailed information, the reader is referred to Ref. 8.

III. NUMERICAL CALCULATIONS

Dielectronic recombination from a H-like ground state to a state of a He-like ion can be represented by



In the present work, we concentrate on the double-excited states with $n=2$ and $n'=2,3$ only. In order to study the effects of relativity and configuration interaction, we carried out calculations using (1) nonrelativistic single-configuration Hartree-Fock (HF), (2) nonrelativistic multiconfiguration Hartree-Fock (MCHF), (3) multiconfiguration Dirac-Fock¹² with Coulomb interaction for the Auger operator (MCDF-C), and (4) multiconfiguration Dirac-Fock with Coulomb-Breit operator for the Auger calculations (MCDF-B). The nonrelativistic results were obtained by using the nonrelativistic limit of the relativistic model which can be achieved by increasing the velocity of light a thousand-fold.¹²

The atomic energy levels and bound-state wave functions were calculated using the MCDF atomic structure code in the averaged-level scheme.¹² The effects of quantum electrodynamic corrections, finite nuclear size, and relaxation were included in the relativistic calculations of transition energies. The detailed Auger and $E1$ radiative rates for each autoionizing state were computed according to Eqs. (4), (5), and (6). For nonrelativistic calculations, we included only the Coulomb interaction in the treatment of Auger transitions.

IV. RESULTS AND DISCUSSION

The detailed Auger and radiative rates for the doubly excited He-like autoionizing states were calculated for the Ne^{8+} , Cr^{22+} , Mo^{40+} , and Xe^{52+} ions. The results for the Auger rates are shown in Figs. 1-4. For some au-

toionizing states (e.g., $2s^2^1S_0$, $2p^2^1S_0$, and $2p3p^1D_2$), the effect of configuration interaction could change the Auger rates by as much as a factor of 5. Relativistic effects on Auger transitions can arise from (1) changes in energies, (2) shifts in wave functions, (3) spin-orbit interaction, and (4) magnetic and retardation corrections in the two-electron operator. Of all these factors, spin-orbit interaction and magnetic and retardation interaction can change the individual rates by as much as a factor of 3 for medium- Z ions (Fig. 3). For the $2p^2(^3P)$, $2p3p(^1P, ^3P)$, and $2p3d(^1D, ^3D)$ states, Auger decays are forbidden in LS coupling. The Auger transitions of these states become possible due to the inclusion of spin-orbit mixing and Breit interaction.

In our present work, the contributions of the Breit interaction to the Auger rates are generally quite small except for the $2s^2(^1S_0)$ and $2s2p(^1P, ^3P)$ states. For the $2s^2(^1S_0)$ and $2s2p(^3P_0)$ states, the Breit interaction increases the Auger rates by 30% and a factor of 4, respectively. This is consistent with the finding for the K - LL Auger rates in neutral atoms.¹³

In Fig. 5 the radiative rates for the $2s^2-1s2p$ transitions are displayed. The $E1$ transition for this state is forbidden in the single-configuration calculation. The $E1$ radi-

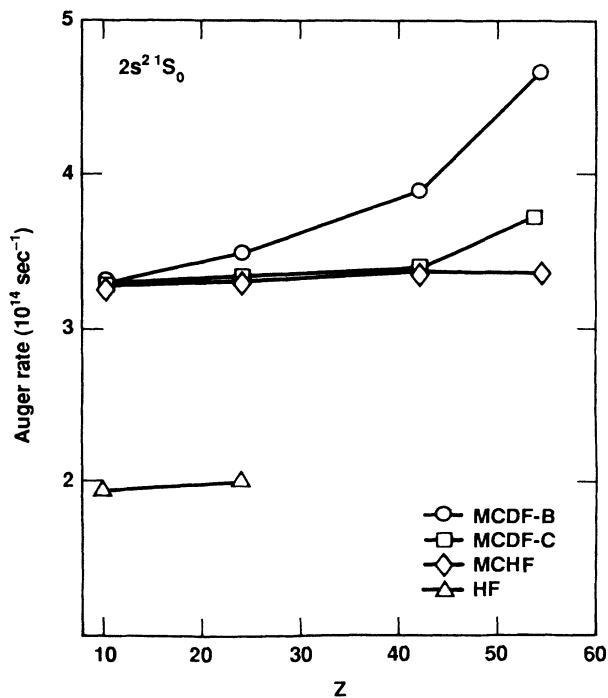


FIG. 1. Auger rates for the $2s^2^1S_0$ state as functions of atomic number. The circles indicate the results from multiconfiguration Dirac-Fock model with the Coulomb-Breit operator for the Auger calculations (MCDF-B). The squares represent the values from the MCDF model with Coulomb interaction for the Auger calculations (MCDF-C). The diamonds are the results from the nonrelativistic multiconfiguration Hartree-Fock (MCHF) and the triangles indicate the predictions from the single-configuration Hartree-Fock model (HF). The lines are drawn to guide the eyes.

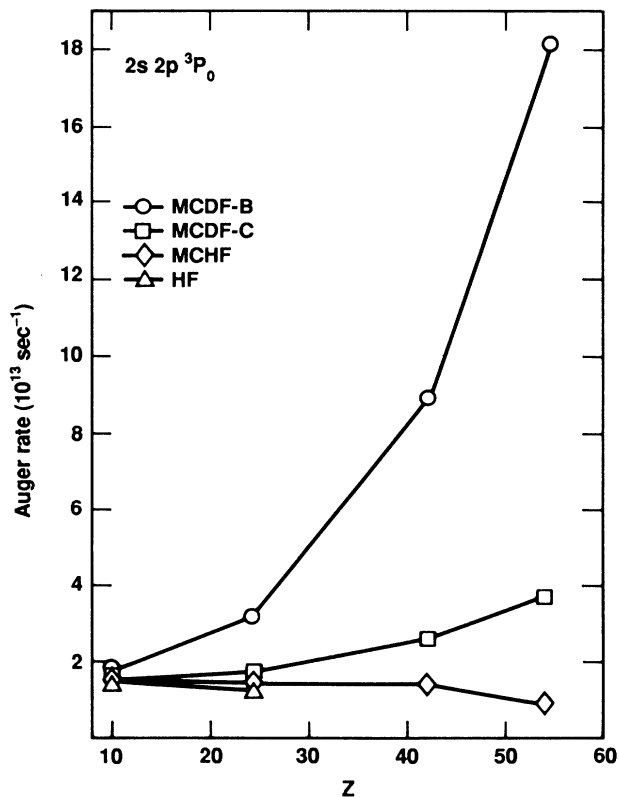


FIG. 2. Auger rates for the $2s2p^3P_0$ state as functions of atomic number. The legends are the same as Fig. 1.

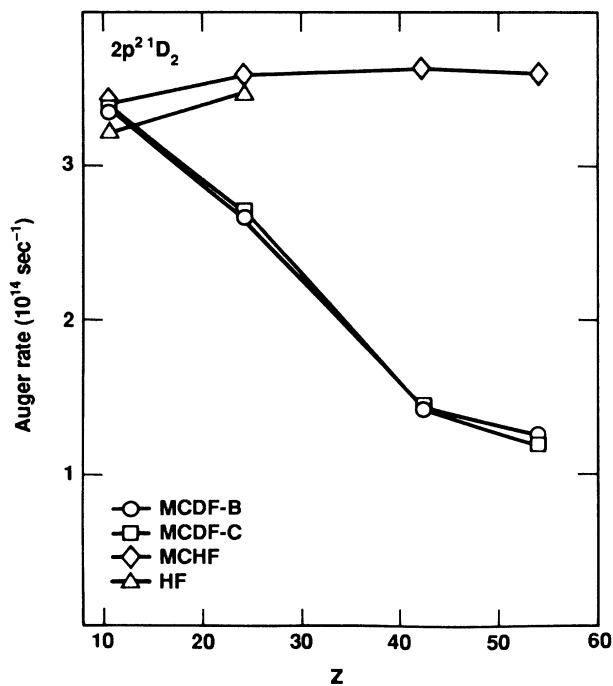


FIG. 3. Auger rates for the $2p^2^1D_2$ state as functions of atomic number. The legends are the same as in Fig. 1.

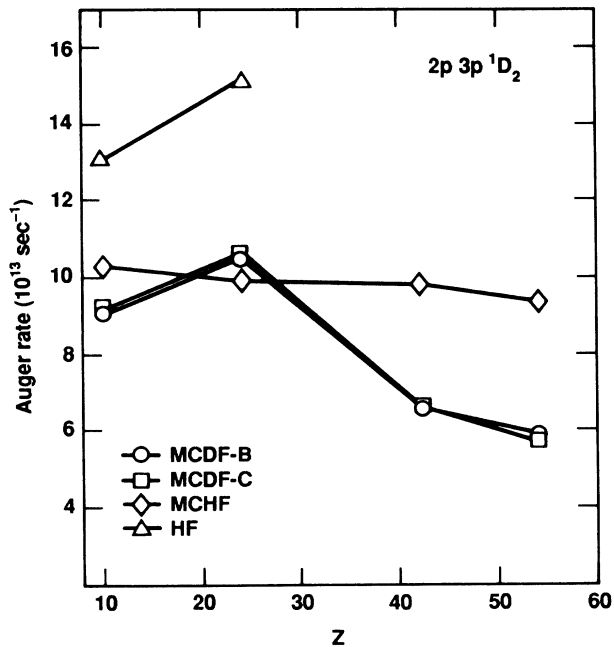


FIG. 4. Auger rates for the $2p3p^1D_2$ as functions of atomic number. The legends are the same as Fig. 1.

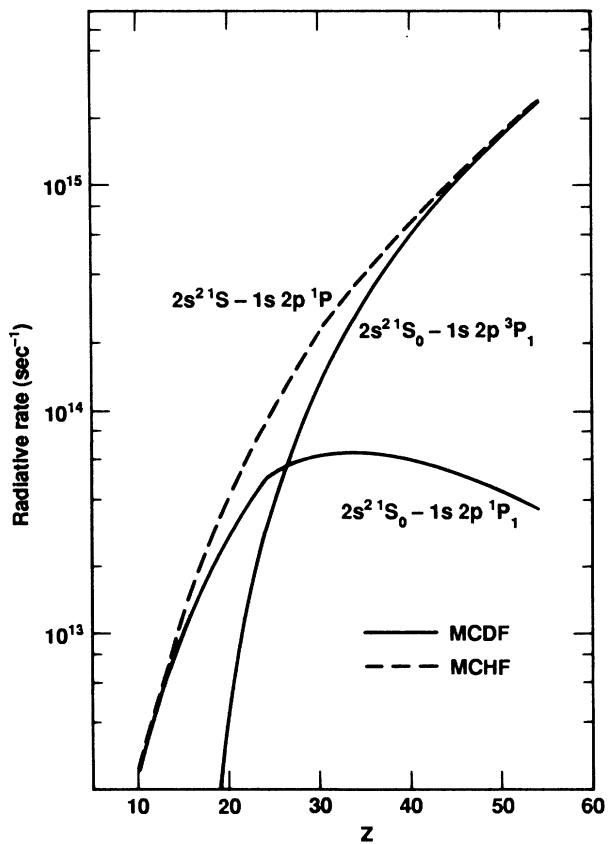


FIG. 5. Radiative rates for the $2s^2-1s2p$ transitions as functions of atomic number. The solid curves indicate the results from the MCDF model. The dashed curve represents the predictions from the MCHF calculations.

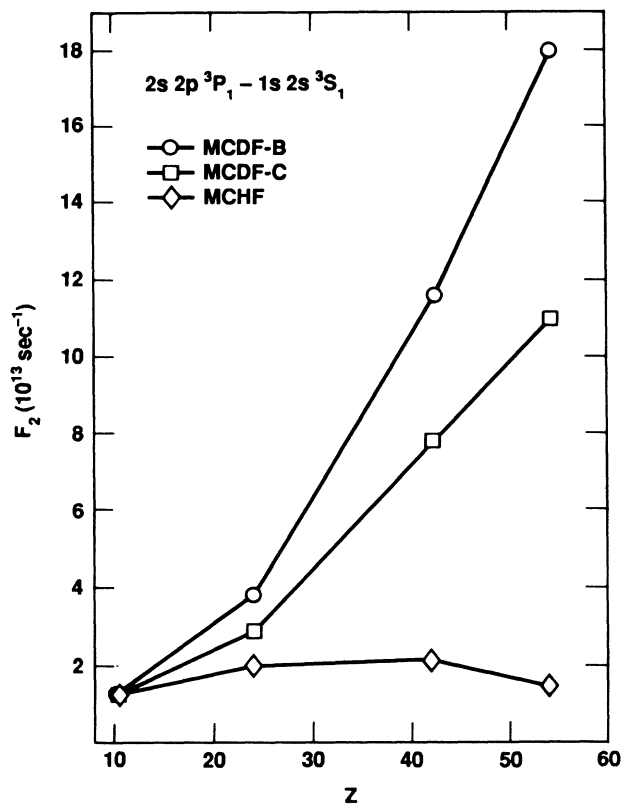


FIG. 6. The F_2 values for the $2s2p^3P_1 - 1s2s^3S_1$ transition as functions of atomic number. The legends are the same as in Fig. 1.

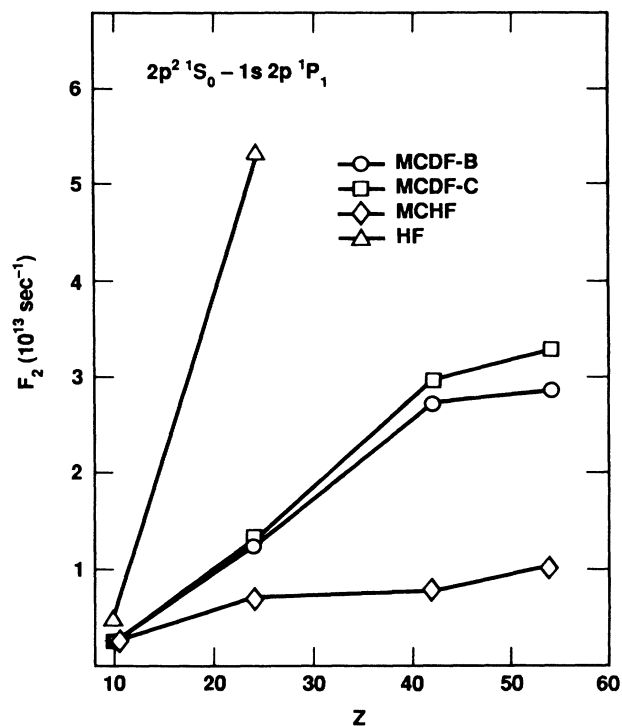


FIG. 7. The F_2 values for the $2p^2^1S_0 - 1s2p^1P_1$ transition as functions of atomic number. For legends refer to Fig. 1.

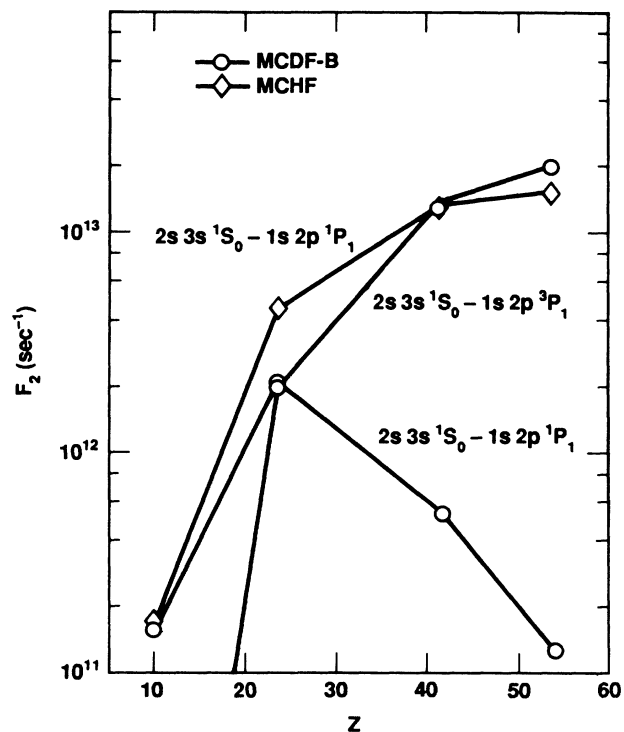


FIG. 8. The satellite intensity factor F_2 for the $2s3s-1s2p$ transitions as functions of atomic number. The legends are the same as in Fig. 1.

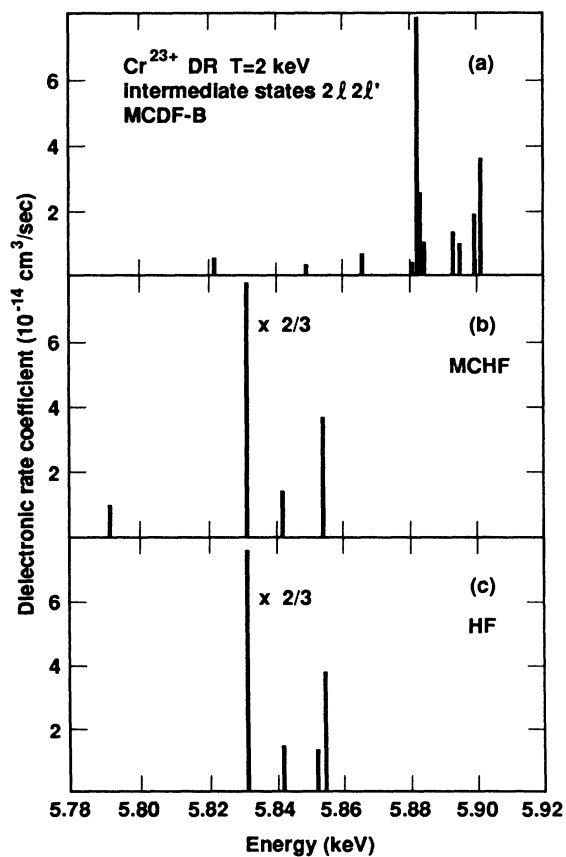


FIG. 9. The dielectronic satellite spectra for the Cr^{23+} ion via intermediate $2l2l'$ states for the electron temperature $T=2$ keV. (a) shows the results from the MCDF-B model. (b) and (c) represent the predictions from the MCHF and HF, respectively.

TABLE I. Radiative rates $A_r(d-f)$, Auger rates $A_a(d)$ and $F_2(d-f)$ for some states of $2l2l'$ and $2l3l'$ configurations of He-like chromium. All rates and F_2 values are in units of 10^{13} sec^{-1} .

Upper states $ d\rangle$	Lower states $ f\rangle$	$A_r(d-f)$		$A_a(d)$		$F_2(d-f)$	
		HFS	MCDF-B	HFS	MCDF-B	HFS	MCDF-B
$2s^2^1S_0$	$1s2p^1P_1$	5.18	4.89	31.39	34.84	2.07	2.01
$2p^2^3P_2$	$1s2p^3P_1$	11.93	11.65	8.16	8.63	4.95	5.21
$2p^2^1D_2$	$1s2p^1P_1$	34.06	32.19	28.15	26.71	34.63	32.52
$2p^2^3P_0$	$1s2p^3P_1$	38.57	37.14	0.26	0.29	0.13	0.14
$2p^2^1S_0$	$1s2p^1P_1$	35.82	34.21	3.33	2.68	1.52	1.24
$2s2p^3P_0$	$1s2s^3S_1$	19.94	20.04	1.37	3.16	0.64	1.36
$2s2p^3P_1$	$1s2s^3S_1$	19.53	19.48	1.76	3.01	2.38	3.82
$2s2p^3P_2$	$1s2s^3S_1$	20.08	19.83	1.37	1.58	3.21	3.66
$2s2p^1P_1$	$1s2s^1S_0$	19.70	19.48	18.62	18.73	14.19	14.14
$2p3s^1P_1$	$1s2s^1S_0$	1.52	1.66		8.09	0.71	0.84
$2s3d^3D_2$	$1s2p^3P_1$	0.93	1.07		2.33	0.53	0.62
$2p3p^1D_2$	$1s2p^1P_1$	3.84	3.55		10.49	3.29	3.07
$2s3s^1S_0$	$1s2p^3P_1$	0.34	0.53		16.77	0.12	0.20
$2p3d^1F_3$	$1s3d^1D_2$	12.30	11.33		2.00	3.28	3.53
$2p3p^1D_2$	$1s3p^1P_1$	16.14	12.81		10.49	13.82	11.05
$2p3s^1P_1$	$1s3s^1S_0$	12.13	11.96		8.09	5.65	6.05
$2s3d^1D_2$	$1s3p^3P_1$	5.86	5.23		2.25	1.55	2.61
$2s3s^1S_0$	$1s3p^1P_1$	3.48	2.40		16.77	1.23	0.90

tive decays of the $2s^2^1S_0$ state were made possible by the strong configuration interaction between $2s^2^1S_0$ and $2p^2^1S_0$ states. Similarly, the $2s3s$ and $2s3d$ states pick up the $E1$ radiative strength to the K shell through the configuration interaction with the $2p3p$ states.

The theoretical results for the satellite intensity factor

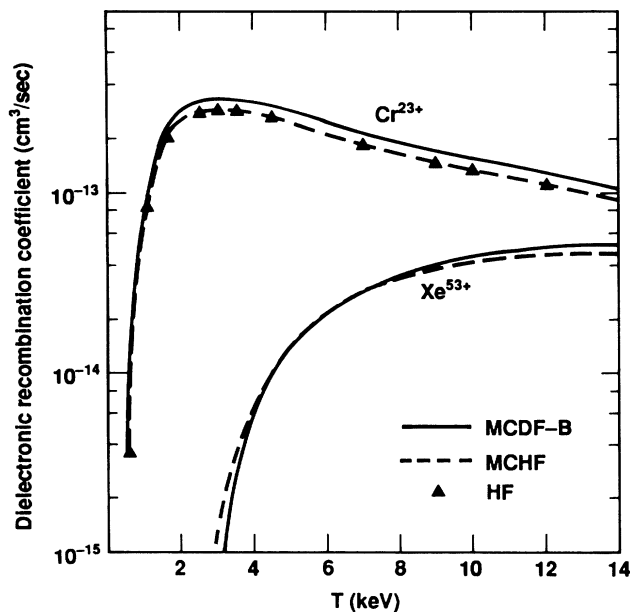


FIG. 10. Total dielectronic recombination rate coefficients for the Cr^{23+} and Xe^{53+} ions as functions of the electron temperature. The solid curves show the results from the MCDF-B model. The dashed curves indicate the values from the MCHF calculations and the triangles represent the predictions from the HF model.

F_2 [Eq. (3)] are compared in Figs. 6–8. From these comparisons, one observed that the effect of configuration interaction can drastically change the intensity factors for some transitions. Furthermore, the Breit interaction can also alter the F_2 values by as much as a factor of 4 at $Z = 54$. In the nonrelativistic single-configuration calculations, the strength of the DR satellite lines concentrates on a few lines. The DR satellite spectra becomes much more complex due to the inclusion of configuration interaction and relativistic effects (see Fig. 9).

In Table I, the radiative rates, Auger rates and F_2 values for the He-like chromium from the present work are compared with the results from nonrelativistic Hartree-Fock-Slater (HFS) calculations,⁴ which included the effects of configuration interaction and spin-orbit mixing. In general, there is good agreement between the two theories. The large discrepancies for the Auger rates and F_2 values of the $2s2p(^3P_0, ^3P_1)$ states are due to the inclusion of the Breit interaction in our Auger calculations. For the $2l3l'$ autoionizing states, deviation up to 50% exists because of the differences in the atomic wave functions.

The total dielectronic recombination coefficients for the Cr^{23+} and Xe^{53+} ions are shown in Fig. 10. The effect of configuration interaction on the total DR rate is rather small. The relativistic effect changes the total DR rates by amounts less than 20%.

We conclude that the effects of configuration interaction and relativity are very important in calculations of the dielectronic satellite spectra. For the light ions, nonrelativistic calculations in intermediate coupling with configuration interaction may be sufficient. However, for the medium-heavy and heavy ions, *ab initio* relativistic calculations in intermediate coupling with configuration interaction including the Breit interaction are necessary.

On the other hand, the total rate coefficient being a sum is much less sensitive to the effects of relativity and electron correlation. It can, generally, be evaluated by using nonrelativistic model except for very heavy ions.

Work performed under the auspices of the U.S. Department of Energy by the Lawrence Livermore National Laboratory under Contract No. W-7405-ENG-48.

¹H. P. Summers, Mon. Not. R. Astron. Soc. **169**, 663 (1974).

²B. L. Whitten, A. U. Hazi, M. H. Chen, and P. L. Hagelstein, Phys. Rev. A **33**, 2171 (1986).

³C. P. Bhalla and K. R. Karim, Phys. Rev. A **34**, 3525 (1986).

⁴K. R. Karim and C. P. Bhalla, Phys. Rev. A **34**, 4743 (1986).

⁵L. A. Vainshtein and U. I. Safronova, At. Data Nucl. Data Tables **21**, 49 (1978).

⁶J. Nilsen, At. Data Nucl. Data Tables **37**, 191 (1987).

⁷M. J. Seaton and P. J. Storey, in *Atomic Processes and Applications*, edited by P. G. Burke and B. L. Moiseiwitsch (North-Holland, Amsterdam, 1976), p. 133.

⁸M. H. Chen, Phys. Rev. A **31**, 449 (1985).

⁹W. Bambynek, B. Crasemann, R. W. Fink, H. U. Freund, H. Mark, C. D. Swift, R. E. Price, and P. V. Rao, Rev. Mod. Phys. **44**, 716 (1972).

¹⁰B. J. McKenzie, I. P. Grant, and P. H. Norrington, Comput. Phys. Commun. **21**, 233 (1980).

¹¹I. P. Grant, J. Phys. B **7**, 1458 (1974).

¹²I. P. Grant, B. J. McKenzie, P. H. Norrington, D. F. Mayers, and N. C. Pyper, Comput. Phys. Commun. **21**, 207 (1986).

¹³M. H. Chen and B. Crasemann, Phys. Rev. A **28**, 2829 (1983).